



# Algorithm Theoretical Basis Document for MTG OSISAF Sea Surface Temperature

Product OSI-206-b

Version: 0.3  
Date: 18/11/2019  
Prepared by S. Saux Picart  
Météo France/CMS



## Documentation change record

Version	Date	Authors	Description
<b>0.1</b>	27/3/2017	M-F/CMS	Initial submitted version
<b>0.2</b>	5/5/2017	M-F/CMS	Modifications in response to PDCR RIDs: <ul style="list-style-type: none"> <li>• RID_025: Text added in section 1 stating the targeted application and reference to validation report of MSG to assess validation of MTG products against.</li> <li>• RID_032: Clarification of the SST correction scheme in section 3.2</li> <li>• RID_047: Description of the remapping process added in section 4.</li> </ul>
<b>0.3</b>	18/11/2019	M-F/CMS	Minor correction in Section 2.1 and Table 2: Change time interval for calculating temporal variability indicator.

# Contents

<b>1</b>	<b>Introduction</b>	<b>4</b>
1.1	Reference documents . . . . .	4
1.2	Applicable documents . . . . .	4
1.3	Purpose and scope of the document . . . . .	4
1.4	Scientific background . . . . .	4
1.5	Characteristics of MTG/FCI instrument . . . . .	5
1.6	Acronyms and definitions . . . . .	5
<b>2</b>	<b>Overview of the processing</b>	<b>7</b>
2.1	The main steps of the processing . . . . .	7
2.2	Data . . . . .	7
2.2.1	MTG/FCI data . . . . .	8
2.2.2	Dynamic ancillary data . . . . .	8
2.2.3	Auxillary datasets . . . . .	8
2.3	Quality level and test indicators . . . . .	8
2.4	Products . . . . .	10
<b>3</b>	<b>SST algorithm</b>	<b>11</b>
3.1	Non-linear SST algorithm . . . . .	11
3.2	Brightness temperature simulation and adjustment . . . . .	12
3.2.1	Brightness temperature simulation . . . . .	12
3.2.2	Brightness temperature simulation adjustment . . . . .	12
3.3	Corrected SST . . . . .	13
3.4	Saharan dust correction . . . . .	14
<b>4</b>	<b>Hourly synthesis</b>	<b>16</b>
<b>5</b>	<b>Single Sensor Error Statistics</b>	<b>16</b>
<b>6</b>	<b>Continuous control and validation plan</b>	<b>17</b>
6.1	Control . . . . .	17
6.2	Validation plan . . . . .	17
6.2.1	The Matchup DataSet (MDS) . . . . .	17
6.2.2	Statistics . . . . .	18

## List of Figures

1	Channels of FCI instrument. . . . .	6
2	Storage field of brightness temperature difference (simulation - observation) for one slot (left) and adjustment field for IR 10.8 of MSG/SEVIRI (right) produced by accumulating and smoothing storage fields between 00h UTC $\pm$ 3h. . . . .	13
3	Example of algorithm correction field for MSG/SEVIRI SST reprocessing. . . . .	14
4	Illustration of the decontamination/drift of the BT 3.9 $\mu$ m for Meteosat 10 (red line). Extracted from the Global Space-based Inter-Calibration System ( <a href="http://gsics.wmo.int/">http://gsics.wmo.int/</a> )	15
5	Control of the BT adjustment for channel 10.8 (left) and 12.0 (right) $\mu$ m. Temporal evolution (2005) of the difference, in K, between simulated and observed BT in green; and between adjusted simulated and observed BT in red (global mean and standard deviation). Top: daytime; Bottom: night-time. Computed from MSG/SEVIRI reprocessing data. . . . .	18
6	Example of maps of binned differences $SST_{sat} - SST_{insitu}$ from MSG/SEVIRI reprocessing validation. . . . .	19
7	Example of dependence plots from MSG/SEVIRI reprocessing validation. The difference $SST_{sat} - SST_{insitu}$ is plotted as a function of different variables of interest. . . . .	20

## List of Tables

1	Extracted from [AD.1]. Threshold, target and optimal accuracies define respectively: the lower limit of usefulness, the main reference for assessment at EUMETSAT and the optimal performance reachable in theory provided the instrument characteristics . . . . .	5
2	List of indicators contributing to the quality level . . . . .	9

# 1 Introduction

The EUMETSAT Satellite Application Facilities (SAFs) are dedicated centres of excellence for processing satellite data. They form an integral part of the distributed EUMETSAT Application Ground Segment. The Ocean and Sea Ice SAF, led by Météo-France/Centre de Météorologie Spatiale (M-F/CMS), has the responsibility of developing, validating and distributing near real time products of Sea Surface Temperature (SST), radiative fluxes, wind and Sea Ice for a variety of platforms/sensors.

As part of the Third Continuous Development and Operations Phase (CDOP-3) OSI SAF (more specifically M-F/CMS) has committed to provide user community with operational Day 1 product of Sea Surface Temperature and Radiative Fluxes from Meteosat Third Generation Flexible Combined Imager (MTG/FCI).

SST MTG products are designed to answer the need of the scientific and meteorological communities in several domains such as regional NWP, oceanography and operational oceanography or fisheries.

## 1.1 Reference documents

Ref	Title	Code
[RD.1]	Operational SST retrieval from MSG/SEVIRI and GOES-E upgraded chain, validation report	SAF/OSI/CDOP/M-F/TEC/MA/183
[RD.2]	Algorithm Theoretical Basis Document for the Cloud Product Processors of the NWC/GEO MTG-I day-1, version 10d	NWC/CDOP2/MTG/MFL/SCI/ATBD/Cloud

## 1.2 Applicable documents

Ref	Title	Code
[AD.1]	OSI SAF, Product Requirement Document version 3.7	SAF/OSI/CDOP2/M-F/MGT/PL/2-001
[AD.2]	MTG End-User Requirements Document [EURD] version v3C	EUM/MTG/SPE/07/0036

## 1.3 Purpose and scope of the document

This document describes the foreseen algorithms and methods to be implemented for production of MTG/FCI SST product OSI-206-b with the required specifications (see table 1), it also gives a brief overview of the processing chain and of the datasets to be used for the sake of clarity.

This document is written in the framework of the Preliminary and Design Component Consolidation Review for MTG/FCI SST and radiative fluxes. All the methods and parameter values given in the following are the best guess we can make today based on past experience. They may vary in the next few years preceding the launch of MTG and once real MTG/FCI data are available after MTG-I1 launch.

## 1.4 Scientific background

SST retrieval from infrared (IR) radiometer measurements classically uses multichannel algorithms (e.g. McCain et al., 1985). More recent developments have improved retrieval through the usage of atmospheric profiles of temperature and water vapour provided by Numerical Weather Prediction (NWP) models in order to correct for regional and seasonal biases. OSI SAF (at M-F/CMS) has long term experience in using the algorithm correction method in the newer

Table 1: Extracted from [AD.1]. Threshold, target and optimal accuracies define respectively: the lower limit of usefulness, the main reference for assessment at EUMETSAT and the optimal performance reachable in theory provided the instrument characteristics

Product ID	Spatial coverage	Spatial sampling	Threshold accuracy. Monthly bias, STD	Target accuracy. Monthly bias, STD	Optimal accuracy. Monthly bias, STD
OSI-206-b	60°N to 60°S and 60°W – 60°E	0.05°	1°C, 1.5°C	0.5°C, 1°C	0.1°C, 0.5°C

processing chains for MSG/SEVIRI and Metop/AVHRR. This method developed by Le Borgne et al. (2011) uses NWP output together with a guess SST (analysis) and a radiative transfer model to simulated Brightness Temperatures (BT) for each pixels. It then uses this information to compute a so-called simulated SST using the multichannel algorithm to be corrected for regional and seasonal biases. Under some conditions and hypothesis, the difference between guess SST and simulated SST is the algorithm error with respect to specific atmospheric conditions.

Another similar approach have been developed by Merchant et al. (2008) and further enhanced in Merchant et al. (2013). It is also based on NWP data and simulation of BTs. An inversion method is used to explain the differences between simulated and observed BTs in terms of SST correction.

Both methods aforementioned requires a step of adjustment of the simulated BTs. This step is designed to ensure that simulated BTs are not biased by uncertainties in the radiative transfer model used and its inputs.

As of today there is no consensus about the best possible method and unless new progress is made in the next few years, OSI SAF is going to keep on using the algorithm correction method as it is done today. Operational processing chains for MSG/SEVIRI and Metop/AVHRR using this method have shown good and consistent results. However, whatever the method, SST estimations from IR data is strongly dependant on the cloud mask used.

MTG products quality will be assessed with respect to the product requirements [AD.1] and the validation results obtained for operational MSG processing [RD.1].

## 1.5 Characteristics of MTG/FCI instrument

The Flexible Combined Imager (FCI) performs radiometric measurements in sixteen channels: five in the visible region of the spectrum, three in the near infrared and eight in the infrared (Figure 1). The spatial resolution at the satellite sub-point is 1 km for visible and near infrared channels and 2 km for infrared channels. The full disk is scanned with a basic repeat cycle of 10 minutes [AD.2].

## 1.6 Acronyms and definitions

The term workfile is used to designate intermediary files produced by the processing chain. Workfiles contains most of the intermediate variables of the processing.

AOD	Aerosol Optical Depth
AVHRR	Advanced Very High Resolution Radiometer
BT	Brightness Temperature

CHANNEL	CENTRE WAVELENGTH	SPECTRAL WIDTH	SPATIAL SAMPLING DISTANCE (SSD)
VIS 0.4	0.444 $\mu\text{m}$	0.060 $\mu\text{m}$	1.0 km
VIS 0.5	0.510 $\mu\text{m}$	0.040 $\mu\text{m}$	1.0 km
VIS 0.6	0.640 $\mu\text{m}$	0.050 $\mu\text{m}$	1.0 km; 0.5 km*
VIS 0.8	0.865 $\mu\text{m}$	0.050 $\mu\text{m}$	1.0 km
VIS 0.9	0.914 $\mu\text{m}$	0.020 $\mu\text{m}$	1.0 km
NIR 1.3	1.380 $\mu\text{m}$	0.030 $\mu\text{m}$	1.0 km
NIR 1.6	1.610 $\mu\text{m}$	0.050 $\mu\text{m}$	1.0 km
NIR 2.2	2.250 $\mu\text{m}$	0.050 $\mu\text{m}$	1.0 km; 0.5 km*
IR 3.8 (TIR)	3.800 $\mu\text{m}$	0.400 $\mu\text{m}$	2.0 km; 1.0 km*
WV 6.3	6.300 $\mu\text{m}$	1.000 $\mu\text{m}$	2.0 km
WV 7.3	7.350 $\mu\text{m}$	0.500 $\mu\text{m}$	2.0 km
IR 8.7 (TIR)	8.700 $\mu\text{m}$	0.400 $\mu\text{m}$	2.0 km
IR 9.7 (O <sub>3</sub> )	9.660 $\mu\text{m}$	0.300 $\mu\text{m}$	2.0 km
IR 10.5 (TIR)	10.500 $\mu\text{m}$	0.700 $\mu\text{m}$	2.0 km; 1.0 km*
IR 12.3 (TIR)	12.300 $\mu\text{m}$	0.500 $\mu\text{m}$	2.0 km
IR 13.3 (CO <sub>2</sub> )	13.300 $\mu\text{m}$	0.600 $\mu\text{m}$	2.0 km

Figure 1: Channels of FCI instrument.

ECMWF	European Centre for Medium-range Weather Forecasts
FCI	Flexible Combined Imager
FDC	Full Disk Coverage
FDHSI	Full Disk High Spectral resolution Imagery
GDS	GHRSSST Data Specification
GHRSSST	Group for High Resolution SST
GTS	Global Telecommunication System
IR	Infrared
M-F/CMS	Météo-France/Centre de Météorologie Spatiale
MDS	Matchup DataSet
MSG	Meteosat Second Generation
MTG	Meteosat Third Generation
Metop	Meteorological Operational
NWP SAF	Numerical Weather Prediction Satellite Application Facility
OSI SAF	Ocean and Sea Ice Satellite Application Facility
OSTIA	Operational Sea Surface Temperature and Sea Ice Analysis
QL	Quality Level
RTM	Radiative Transfer Model
RTTOV	Radiative Transfer for TOVS
SAF	Satellite Application Facility
SDI	Saharan Dust Index
SEVIRI	Spinning Enhanced Visible and InfraRed Imager
SSES	Sensor Specific Error Statistics
SST	Sea Surface Temperature
TIROS	Television Infrared Observation Satellite
TOVS	TIROS Operational Vertical Sounder

## 2 Overview of the processing

In this section a brief overview of the input datasets used and the main steps of the processing are given.

### 2.1 The main steps of the processing

The processing can be divided into a few main steps:

1. *Simulations of BT*: A Radiative Transfer Model (RTM) will be used for computing simulated BTs for every clear sky sea and lake pixels and for each IR channel used for SST retrieval and every three hours. Currently we use Radiative Transfer for TOVS (RTTOV, Saunders et al. (1999)) version 11. Inputs to this RTM include forecasts of atmospheric profiles of water vapour from a NWP model and a guess SST.
2. *BTs adjustment*: This step is of primary importance because it is designed to ensure that the simulated BTs are not biased by uncertainties in the RTM and its input data. See section 3.2.2 for details.
3. *Saharan Dust Index (SDI)*: It is used for downgrading the quality level of pixels contaminated by atmospheric dust aerosols (see section 2.3) and possibly correcting retrieved SST (see section 3.4).
4. *Control of the mask*: This step is designed to detect possible problems such as remaining cloud contamination. It consists in a series of tests which are contributing to the Quality Level (QL) assignment (see section 2.3). These tests are performed at various stage of the processing depending on the tested values.
5. *SST retrieval*: A classical non-linear SST algorithm is used to provide a first estimate of the SST (see section 3.1). It is used in particular in the control of the mask.
6. *SST algorithm corrections*: Le Borgne et al. (2011) algorithm correction scheme is used (section 3.3) to reduce regional and seasonal biases.
7. Computation of *Single Sensor Error Statistics (SSES)*
8. Production of *hourly synthesis* and *GHRSSST compliant L3C product* from 10 minutes workfiles.

These steps are not applied in a sequential order, in fact they are not even performed with the same time step. Simulation of BTs are performed every three hours as NWP forecasts are produced on a three-hourly basis. BT adjustment field is computed on daily basis, they are used to elaborate the algorithm correction fields every three hours. Hourly synthesis are computed at round hours. The hourly synthesis for  $H$  includes SST computed at all slots in the interval  $[H - 30, H + 20]$ . However, please note that the production of SST for the slots in the interval  $[H - 30, H + 20]$  necessitate the reception of the slots within the interval  $[H - 50, H + 40]$ , see section 2.3 for clarification (table 2, SST temporal variability).

### 2.2 Data

The data used in the processing are listed below. They are described in their version available at the time of the writing of this document. It is likely that this list will evolve in the future to make use of the best dataset available.

### 2.2.1 MTG/FCI data

Input data for the processing chain consist in MTG FCI level 1 Full Disk Coverage (FDC) data at Full Disk High Spectral resolution Imagery (FDHSI): Brightness temperature at 3.8, 8.7, 10.5, 12.4 and 13.3 $\mu$ m.

### 2.2.2 Dynamic ancillary data

- 3-hourly atmospheric temperature and humidity profiles (plus a few surface fields) from NWP model. Nowadays European Centre for Medium-Range Weather Forecasts (ECMWF) data are used in SST operational chains.
- An SST analysis is needed for simulations of BTs. Nowadays, this analysis is the OSTIA SST daily analysis (Donlon et al., 2012).
- The cloud mask originates from the Cloud Product Processor of the NWC SAF for MTG which will be run at M-F/CMS [RD.2].

### 2.2.3 Auxillary datasets

These are the static datasets such as climatologies. They include the data being used nowadays by OSI SAF for operational processing.

- Foundation SST climatology. Currently a climatology based on OSTIA daily SST re-analyses (1985-2007) is used (Donlon et al., 2012).
- SST front climatology developed by the University of Rhodes Island.
- Land/Sea/Lake mask: ARC-Lake

## 2.3 Quality level and test indicators

We use the concept of indicator to quantify, in an empirical way, the risk of having an error in the SST retrieval because of uncertainties in algorithms or ancillary variables. For each test, the tested quantity (tested\_value) is compared to a limit value (limit\_value) and to a critical value (critical\_value). Outside this range there is either no problem or the risk of error is too high. The core definition of the test indicator is given below, however many other factors can influence each indicators (for example availability of ancillary data used in the definition of the indicator) that are not detailed here:

$$\text{test\_indicator} = 100(\text{tested\_value} - \text{limit\_value})/(\text{critical\_value} - \text{limit\_value}) \quad (1)$$

There is a range of test\_value, for example: the difference between the climatological SST and the retrieved SST, the SDI, the distance to cloud, etc. [limit\_value, critical\_value] define a range of the test\_value below and above which the test\_indicator is 0 and 100 respectively.

The formulation above has the advantage of homogenising all the indicators on a unique scale:

- 0: no problem
- ]0, 100[: potential problem
- 100: critical problem

There are two types of indicators: (i) the common indicators, independent of the SST retrieved and the algorithm used, they are generic to the whole processing. They include the dust indicator, the distance to cloud indicator and the ice indicator. (ii) The specific indicators, based on the value of the SST retrieved in comparison to climatologies of SST and SST gradients (the SST value indicator and the SST gradient indicator). At the end of the processing all these indicators are combined into one single indicator by means of a weighted average: this is the SST mask indicator.

Two other indicators are defined that do not enter in the SST mask indicator, but are considered for determining the quality level: the indicator reflecting the uncertainties of the SST algorithm with respect the satellite zenith angle (algorithm indicator), and the indicator about the confidence we have in the correction term (the SST correction indicator).

A brief description of the tests is given in table 2:

*Table 2: List of indicators contributing to the quality level*

Test	Description/purpose
SST value	This test aims at attributing a lower quality level to SST values too different from climatology. The local value of estimated SST is compared to a climatology of SST, the larger the difference between estimated SST and SST climatology, the higher the indicator.
SST spatial variability	The main objective of this test is to attribute a lower quality level to pixels in areas where the gradients are unrealistically large due to the presence of undetected cloud cover in most cases. The local value of the SST gradient is compared to a climatology of maximum gradient.
SST temporal variability	The main objective of this test is to attribute a lower quality level to pixels displaying a fast changing SST suggesting that some cloud contamination is occurring, by evaluating the BT change in one IR channel over 30 minutes.
Aerosol dust	This test influences the quality level of pixels contaminated by Saharan dusts. It is directly related to the SDI.
Distance to cloud	Pixels in the immediate vicinity of clouds are likely to be partly covered by cloud or affected by transparent undetected clouds.
Sea ice	The purpose of this test is to degrade the quality of pixels suspected to contain ice.
Satellite zenith angle	The test takes into account the fact that high satellite zenith angle is likely to lead to higher uncertainty because of higher atmospheric optical depth. The resulting indicator is directly linked to the satellite zenith angle.
SST correction	This test is based on the assumption that high SST corrections are associated with high uncertainties. It is directly linked to the value of the SST correction. It is only applied in the algorithm correction method.

Quality levels are designed to help users to filter out data that are not sufficiently good for their applications. It is essential to adopt the recommendation of the GHRSSST formalised through the GDS v2 document. For infrared derived SST six quality levels are defined. 0: unprocessed; 1: cloudy, 2: bad, 3: suspect, 4 acceptable, 5 excellent.

The value of the quality level is determined by examining the values of three indicators: the SST mask indicator (resulting from several sub-indicators as explained above), the algorithm indicator and the SST correction indicator (only in the case of the algorithm correction method, see section 3.3). The poorest indicator will drive the value of the quality level.

## 2.4 Products

As per [AD.1] one product will be delivered by the operational chain:

- hourly level 3 subskin SST on a  $0.05^\circ$  regular grid with a target accuracy of  $0.5^\circ\text{C}$  in bias and  $1^\circ\text{C}$  in standard deviation.

### 3 SST algorithm

In this section we present the “classical” SST algorithm used in the control of the mask, the method for bias correction of SST based on simulation of BTs, and the method envisaged for taking into account atmospheric Saharan dust contamination.

#### 3.1 Non-linear SST algorithm

A classical non-linear SST algorithm will be used to provide a first estimate of the SST. This estimate is used in various steps of the processing, it is referred to as the “classical” SST in the following:

- it is used in the calculation of an initial value of some indicators and QL (see section 2.3).
- it is used in the brightness temperature adjustment step (see section 3.2.2)
- it is the basis of the algorithm correction method (see section 3.3)

Non-linear algorithm have been used for a long time for retrieving SST from BTs in infrared channels (McCain et al., 1985; Walton et al., 1998) measured by a variety of instruments such as AVHRR and SEVIRI. These algorithms have the following generic form:

$$\hat{x} = a_0 + \mathbf{a}^\top \mathbf{y}_0 \quad (2)$$

where,  $\hat{x}$  is the estimated SST,  $a_0$  is an offset coefficient,  $\mathbf{a}$  is a column vector of weighting coefficients and  $\mathbf{y}_0$  contains the observed BTs. The coefficients contained in the vector  $\mathbf{a}$  are potentially functions of SST climatology and satellite zenith angle.

It is likely that the algorithm will have the same form as the one used for MSG/SEVIRI operational processing and reprocessing:

$$\text{SST} = (a + b S_\Theta) T_{10.8} + (c + d S_\Theta + e T_{clim})(T_{10.8} - T_{12.0}) + f + g S_\Theta \quad (3)$$

where,  $S_\Theta = \sec(\Theta)$  and  $\Theta$  is the satellite zenith angle.  $T_{clim}$  is the climatological temperature.

However MTG/FCI channels having slightly different characteristics (centre wavelength, spectral width), the algorithm above may not be optimal. Therefore, the channels used in this retrieval will be picked between the three FCI channels IR 8.7, IR 10.5 and IR 12.3. We are not planning to use IR 3.8 because it is preferable to use the same algorithm for day and night, and IR 3.8 is too near the visible spectrum. It is not possible today to tell which combination of channels will give the best results.

Before launch a study will be carried out on simulated data (RTM simulations using atmospheric profiles) to determine one or more algorithms and their coefficients. One algorithm will be implemented in the chain ready for processing real data as soon as it becomes available. When real data becomes available during commissioning phase the algorithm(s) will be compared to in situ measurements (see section 6) and their coefficients adjusted. At this point the final form of the algorithm and its coefficients will be chosen and implemented in the chain ready for day 1 production. This procedure was already followed in the past for previous instruments when they were first launched.

The term  $(T_{10.8} - T_{12.0})$  in equation 3 (that may be different for MTG) is used in “split-window” algorithms to correct for absorption by water vapour in the atmosphere. However, this term is also particularly sensitive to radiometric noise; it is therefore smoothed over boxes (of a size TBD in which the atmosphere is assumed to be homogeneous) by a Gaussian filter, applied to clear/no ice pixels. This classical procedure reduces the noise in the retrieved SST and will be applied to MTG/FCI.

Since the coefficient of the SST algorithm are established using simulations from RTTOV radiative transfer model and de-biased against in-situ measurements, the retrieved SST is considered to be the sub-skin SST. One could apply a  $-0.17^{\circ}\text{C}$  (Donlon et al., 2002) to get the skin SST. However this offset is only a very rough conversion term valid at large scale for wind speed exceeding  $6\text{ m/s}^{-1}$ .

## 3.2 Brightness temperature simulation and adjustment

### 3.2.1 Brightness temperature simulation

Simulation of BTs are performed for each clear-sky sea or lake pixel using RTTOV. Input variable to RTTOV are described in section 2.2 and summarized here:

- A first guess of SST ( $SST^{guess}$ , which is a SST analysis such as OSTIA daily analysis).
- Atmospheric temperature and humidity profiles from NWP model.
- MTG/FCI filter functions in the infrared channels.

Simulations are performed at the time stamp of the input model data which is 3-hourly and for the channels of interest for SST and SDI computation (see section 3.4).

### 3.2.2 Brightness temperature simulation adjustment

Before their usage in the algorithm correction or in the optimal estimation, BTs must be adjusted to correct for systematic differences with respect the observations. These differences can be due to:

- NWP atmospheric profiles uncertainties
- Profile sampling
- RTTOV uncertainties
- MTG/FCI filter function and calibration uncertainties

In a synthetic way, we use the difference between simulations and satellite observations (spatially and temporally smoothed) and interpret the differences as an adjustment term. The description of the BT adjustment method is provided in detailed in Tomažić et al. (2014) for Metop/AVHRR.

The adjustment method that will be used for MTG/FCI will follow the same general ideas which are adapted and presented hereafter.

The major hypothesis of the BT adjustment is that there is no average bias between the guess SST (used in BTs simulation) and the true SST. It is therefore crucial to properly filter out cases (pixels) where the observed SST cannot be compared with guess SST (for example if there is a diurnal cycle or cloud contamination). Such filtering may include:

- Quality level filtering: only good quality SST retrievals are used ( $QL \geq 4$ )
- Atmospheric dust aerosol filtering based on the dust aerosol indicator
- SST filtering: we ensure that “classical SST” and guess SST are close to each other (less than 1K difference)

- Elimination of cases where there is a risk of diurnal warming. Filter based on wind speed at 10 meters, solar zenith angle ( $\Theta_{sol}$ ) and a threshold on the difference between observed and simulated BTs.
- Only night-time pixels are kept except at high latitude where day-time pixels are allowed if the difference between simulated and observed BT at  $10.8 \mu\text{m}$  is smaller than  $0.5^\circ\text{C}$ .

Filtered data are averaged temporally and spatially every day at 00h UTC using only slots at  $00\text{h UTC} \pm 3\text{h}$  on a 3-dimensional low resolution grid ( $1 \times 1^\circ$ ). An example of such field is shown on figure 2 (left). When computing the BT adjustment, these fields are averaged over 3 days (3 fields) and the result is smoothed out by applying a Gaussian kernel (radius =  $5^\circ$ ,  $\sigma = 2$ ). In order to fill in any remaining gaps, successive smoothing are applied with increasing kernel size. An example of adjustment field is shown on figure 2 (right). One such field is produced for each channels and at 00h UTC every day and used during the following day. Adjustments are then added to BT simulations to produce adjusted BT simulations (3-hourly).

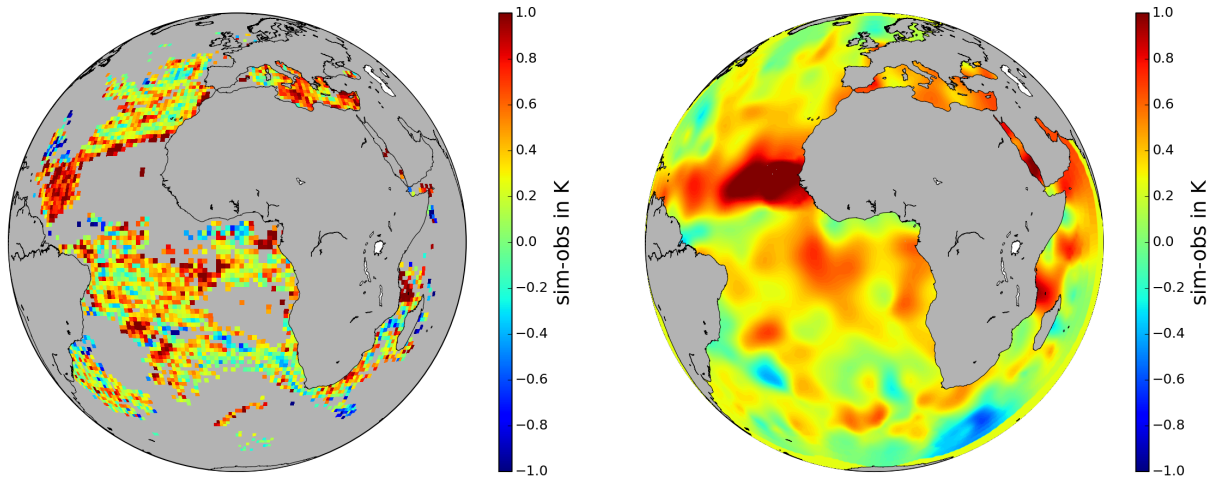


Figure 2: Storage field of brightness temperature difference (simulation - observation) for one slot (left) and adjustment field for IR 10.8 of MSG/SEVIRI (right) produced by accumulating and smoothing storage fields between  $00\text{h UTC} \pm 3\text{h}$ .

### 3.3 Corrected SST

The method of algorithm correction was developed by Le Borgne et al. (2011), it is used today in the operational processing of OSI SAF SST products from Metop-B and MSG/SEVIRI. Operational SST delivered in those products is the corrected SST.

A so-called “simulated” SST ( $SST^{sim}$ ) is computed from simulated BTs adjusted (see section 3.2.2) using the non-linear algorithms described in section 3.1.

The following difference is then computed:

$$\Delta SST = SST^{sim} - SST^{guess} \quad (4)$$

Since the BT simulations used to compute  $SST^{sim}$  have been adjusted to correct for uncertainties linked with RTTOV and atmospheric water vapour profiles,  $\Delta SST$  represent the error due to the algorithm which is unable to cope with all atmospheric conditions.

The corrected SST ( $SST^{cor}$ ) is then computed as follow:

$$SST^{cor} = SST^{obs} - \Delta SST \quad (5)$$

where  $SST^{obs}$  is the “classical” SST as computed by the algorithm presented in section 3.1.

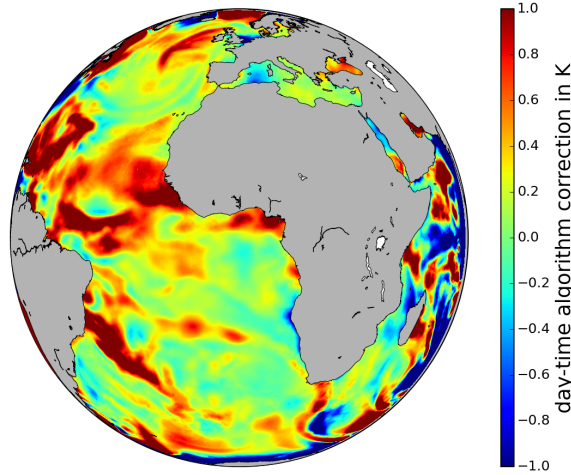


Figure 3: Example of algorithm correction field for MSG/SEVIRI SST reprocessing.

In practice SST algorithm correction fields are computed at the same time step as the simulations (3-hourly) and the correction is linearly interpolated to each slot time.

### 3.4 Saharan dust correction

Saharan dusts in the atmosphere have the effect of attenuating the signal received by the sensor therefore leading to an underestimation of SST. Within MTG disk of view, Saharan dusts are mostly present in the Northern Tropical Atlantic region, in the Mediterranean Sea, in the Red Sea and in the Western part of the Arabic Sea.

The algorithm described in section 3.1 and the method of correction described in section 3.3 do not take into account Saharan dusts. It is therefore essential to correct for such phenomenon, it is generally performed as a post correction once the SST has been calculated.

In MSG/SEVIRI SST processing chain the correction is based on the Saharan Dust Index (Merchant et al., 2006) which is computed for night time with equation 6. During day time, because IR 3.9 is contaminated by sun light, another equation is used (equation 7) and its coefficients are determined locally by regression against night time SDI.

$$SDI_{night} = S_1(T_{3.9} - T_{8.7}) + S_2(T_{10.8} - T_{12.0}) + S_3 \quad (6)$$

$$SDI_{day} = DS_1 T_{8.7} + DS_2 T_{10.8} + DS_3 T_{12.0} + DS_4 T_{13.4} + DS_5 \quad (7)$$

SEVIRI instrument on-board MSG satellites is subject to contamination by the formation of a thin layer of ice on the optic of the instrument. Such contamination is affecting the 3.9  $\mu\text{m}$  which

is used for SDI computation. This problem is visible on the comparison between MSG3/SEVIRI and Metop-A/IASI presented on figure 4. One can observe a gradual contamination (for example between December and July 2013), and a brutal decontamination in July.

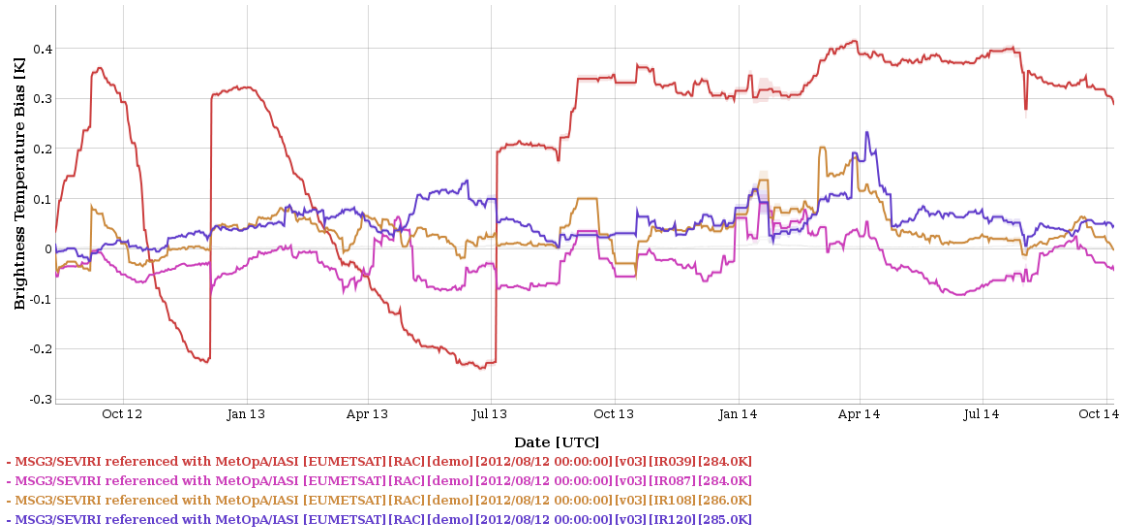


Figure 4: Illustration of the decontamination/drift of the BT 3.9  $\mu\text{m}$  for Meteosat 10 (red line). Extracted from the Global Space-based Inter-Calibration System (<http://gsics.wmo.int/>)

In order to avoid contamination/decontamination phenomenon affecting the SDI, we apply a simple correction to the differences ( $T_{3.9} - T_{8.7}$ ) and ( $T_{10.8} - T_{12.0}$ ) prior to their usage: at midnight the correction term is the median of the difference between simulations and observations of BTS for all clear sky pixels in the domain  $45^\circ\text{S}$  and  $45^\circ\text{N}$ . At any other time, the correction is the one at 0h before.

The SDI correction is based on the definition of a function  $\varphi(\text{SDI})$  that models the average error in SST retrievals due to the presence of Saharan dusts. This function is applied on a pixel basis.

$$\varphi(\text{SDI}) = a_0 + a_1\text{SDI} + a_2\text{SDI}^2 \quad (8)$$

The coefficients are determined by regression using in situ measurements of SST. In order to avoid correcting SSTs where the SDI is not significant, we ensure that below a limit value of SDI, the correction is null. We consider that for SDI below 0, the retrieval of SST is not impacted by Saharan dusts, and therefore no correction is applied.

MTG/FCI channels that would be used to compute SDI are slightly different from MSG/SEVIRI ones. Therefore it is not sure that the SDI computation will be possible at all. We may have to test different combination of channels including the one of Merchant et al. (2006) using three differences of channels ( $T_{3.9} - T_{8.7}$ ,  $T_{3.9} - T_{12.0}$  and  $T_{10.8} - T_{12.0}$  for MSG/SEVIRI channels).

In the case where we would not be able to produce a decent SDI usable to correct SST. We will rely on the forecasts of the MACC project (Monitoring Atmospheric Composition and Climate) to flag pixels where Saharan Dust might have played a significant role. In this case, no correction will be applied but the quality level will be changed according to the value of the Aerosol Optical Depth at 550 nm. This is done already in operational chains of SST for Metop/AVHRR when and where SDI is missing.

## 4 Hourly synthesis

SST is to be computed for every 10 minutes slot going through the processing chain. The intermediate primary workfiles resulting are to be aggregated into hourly workfiles at FDC which are then re-mapped onto a regular  $0.05^\circ$  grid.

To generate hourly synthesis at rounded hour  $H$  all primary workfiles within the time range  $[H - 30, H + 20]$  are used. There is no interpolation and the hourly value attributed to a given pixel is the best available in the time frame, the best being selected based on criteria such as QL or time difference from rounded hour.

Hourly synthesis are then re-mapped as follow: Each quality level is re-mapped separately using a nearest neighbour approach. This results in four fields (QL 2, 3, 4 and 5) at a  $0.05^\circ$  resolution which are combined together giving preference to the higher QL.

## 5 Single Sensor Error Statistics

The SSES are observational error estimates provided at pixel level as a bias and standard deviation as per GHRSSST GDSv2 requirements. They shall be provided per pixel and if possible independently of the QL.

Nowadays for operational SST processing the SSES bias and standard deviation are calculated once for each quality level from analysing differences between full resolution satellite SSTs collocated with drifting buoys available on operational matchup data set. For more information about how this dataset is constructed, please refer to section 6. This process do not give SSES independent of QL and SSES values are static.

Research is ongoing at M-F/CMS to use machine learning approaches for modelling SSES bias and standard deviation. If these research give satisfactory results the method might be implemented in MTG/FCI processing chain.

## 6 Continuous control and validation plan

### 6.1 Control

The aim of a continuous control is to perform in near real time basis (immediately after the production of SST primary workfiles) relevant check to detect a potential problem in the functioning of the chain. The control is performed routinely and does not require in situ data (contrary to the validation, see section 6.2).

It consists in a series of maps and graphics that inform about the successful development of such and such step of the processing chain. The control is performed outside the operational environment, on the workfiles and is not visible to external users. The main steps/variables we plan to monitor are listed below:

- During commissioning phase, MTG/FCI SST products will be compared to MSG/SEVIRI SST products (map of difference, overall bias and standard deviation,...).
- Comparison to other sources of SST (analysis).
- Monitoring of the environmental conditions: SST (analysis), water vapour, solar and satellite zenith angles, wind.
- The adjustment step: in particular we control that the adjustment reduces the differences between observed and simulated BTs.
- The SST correction: we make sure the SST correction is performing well and reduces the differences between retrieved SST and guess SST.

Figure 5 shows an example of the temporal evolution of the difference between simulations and observations before and after adjustment. During night-time, the adjustment brings the difference from approximately  $-0.3\text{K}$  to near zero on average. Whereas during day-time, this difference is brought to around  $0.2\text{K}$ . This is explained by the diurnal variation of the surface temperature, the adjustment being computed using only night-time data.

### 6.2 Validation plan

By opposition to the control, the validation does require external sources of data and synthesis of the results will be available for users of the products through the OSI SAF web site.

#### 6.2.1 The Matchup DataSet (MDS)

All validation procedures require a MDS has been elaborated. In an operational prospective, the MDS gathers in situ SST measurements from ship, moored buoys and drifting buoys available through the Global Telecommunication System (GTS). Collocated full resolution satellite information is added in a 3 hours time frame around the measurement. It consists in all the variables included in the intermediate workfile extracted in a box around the in situ measurements. The MDS for day  $d$  is currently elaborated with a five days delay ( $d+5$ ) to ensure all in situ data are available through GTS. For the purpose of operational validation:

- Only drifter and moored buoys are considered.
- Only the central SST of each box is used.
- Night-time and day-time algorithm are validated separately.

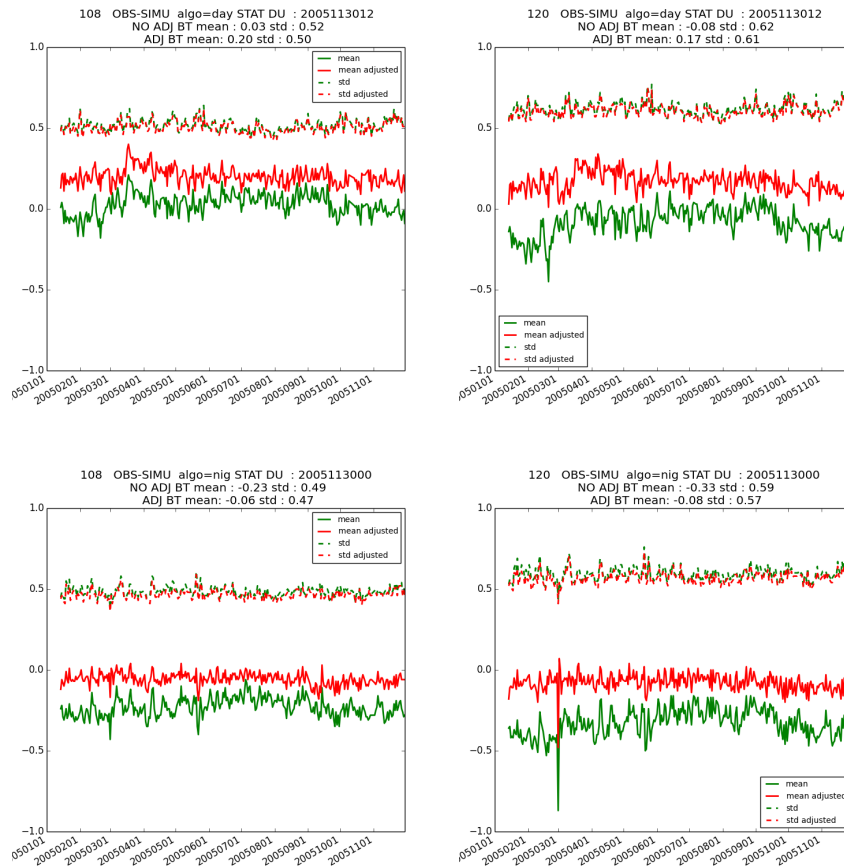


Figure 5: Control of the BT adjustment for channel 10.8 (left) and 12.0 (right)  $\mu\text{m}$ . Temporal evolution (2005) of the difference, in K, between simulated and observed BT in green; and between adjusted simulated and observed BT in red (global mean and standard deviation). Top: daytime; Bottom: night-time. Computed from MSG/SEVIRI reprocessing data.

## 6.2.2 Statistics

To ensure the product satisfies the requirements of [AD.1], statistics are computed routinely (in delayed mode) and manually. They include normal and robust statistics:

- Mean and Standard Deviation of the difference between the retrieved SST and the measurements.
- Median and Robust Standard Deviation (Merchant and Harris, 1999) of the difference between the retrieved SST and the measurements.

Normal statistics are displayed on OSI SAF website, a more thorough analysis is performed and reported in the half yearly status report on OSI SAF activities. A validation report will also be provided for the MTG Operational Readiness Review.

The main characteristics of the validation are:

- Global and regional analysis.
- Productions of maps of binned statistics (on a regular grid and for a time frame). Figure 6 shows a sample of 3-monthly average difference over the entire globe.

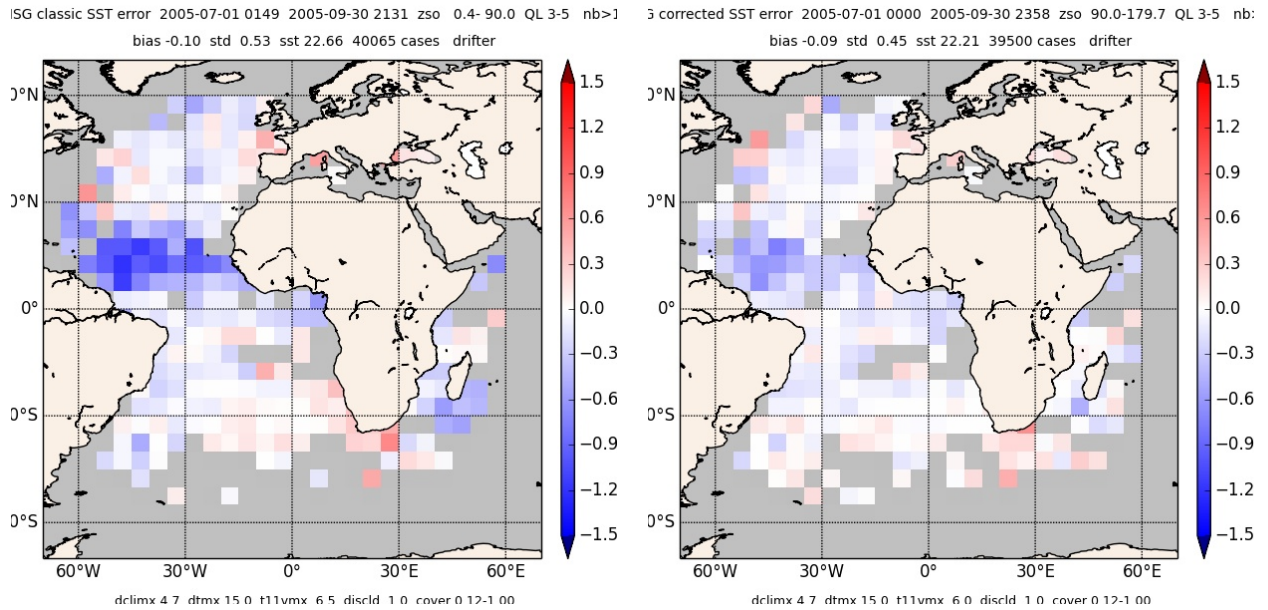


Figure 6: Example of maps of binned differences  $SST_{sat} - SST_{insitu}$  from MSG/SEVIRI reprocessing validation.

- Analysis for different selection criteria, for example based on the quality level or wind speed, etc...
- Analysis of the dependence of the error with respect different variables: latitude, SDI, satellite zenith angle, etc... (see example provided by Figure 7)

MSG corrected SST error 2005-01-01 0000 2005-03-31 2349 zso 90.0-179.3 QL 3-5  
 bias -0.05 std 0.47 sst 22.35 23711 cases drifter  
 dclimx 4.9 dtmx 15.0 t11vmx 4.8 disclcd 1.0 cover 0.12-1.00

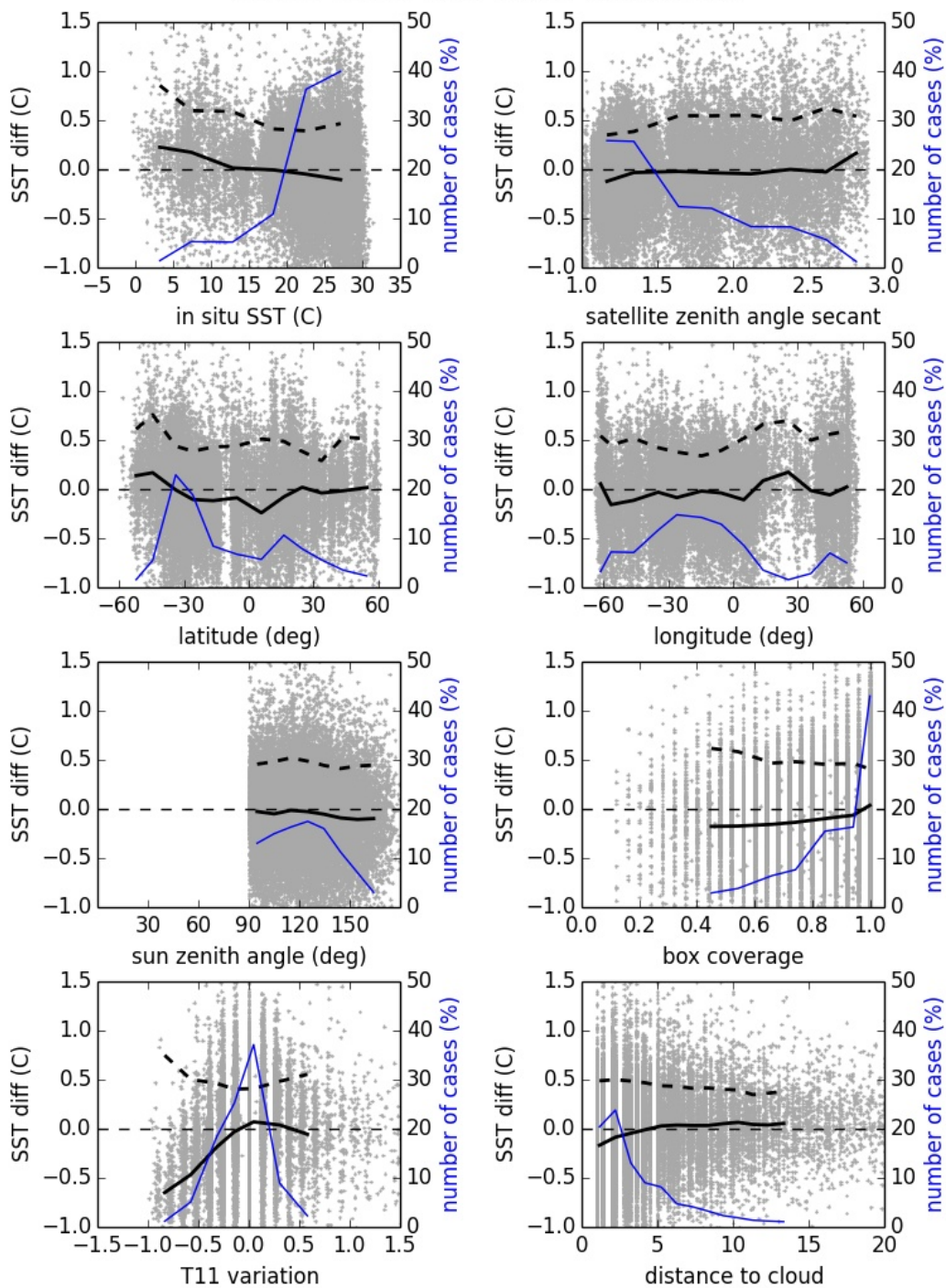


Figure 7: Example of dependence plots from MSG/SEVIRI reprocessing validation. The difference  $SST_{sat} - SST_{insitu}$  is plotted as a function of different variables of interest.

## References

- Donlon, C. J., Martin, M., Stark, J., Roberts-Jones, J., Fiedler, E., and Wimmer, W. (2012). The operational sea surface temperature and sea ice analysis (OSTIA) system. *Remote Sensing of Environment*, 116:140—158.
- Donlon, C. J., Minnett, P. J., Gentemann, C., Nightingale, T. J., Barton, I. J., Ward, B., and Murray, M. J. (2002). Toward improved and validation of satellite and sea surface and skin temperature and measurements and for climate and research. *Journal of Climate*, 15:353–359.
- Le Borgne, P., Roquet, H., and Merchant, C. (2011). Estimation of sea surface temperature from the spinning enhanced visible and infrared imager, improved using numerical weather prediction. *Remote Sensing of Environment*, 115(1):55–65.
- McCain, E. P., Pichel, W. G., and Walton, C. C. (1985). Comparative performance of AVHRR-based multichannel sea surface temperature. *Journal of Geophysical Research*, 90:11587–11601.
- Merchant, C. J., Embury, O., Le Borgne, P., and Bellec, B. (2006). Saharan dust in nighttime thermal imagery: Detection and reduction of related biases in retrieved sea surface temperature. *Remote Sensing of Environment*, 104(1):15–30.
- Merchant, C. J., Filipiak, M. J., Le Borgne, P., Roquet, H., Autret, E., Piollé, J.-F., and Lavender, S. (2008). Diurnal warm-layer events in the western mediterranean and European shelf seas. *Geophys. Res. Lett.*, 35(4):1–4.
- Merchant, C. J. and Harris, A. R. (1999). Toward the elimination of bias in satellite retrievals of skin sea surface temperature 2. comparison with in situ measurements. *Journal of Geophysical Research*, 104(C10):23579–23590.
- Merchant, C. J., Le Borgne, P., Roquet, H., and Legendre, G. (2013). Extended optimal estimation techniques for sea surface temperature from the spinning enhanced visible and infra-red imager (SEVIRI). *Remote Sensing of Environment*, 131:287–297.
- Saunders, R., Matricardi, M., and Brunel, P. (1999). An improved fast radiative transfer model for assimilation of satellite radiance observations. *Quarterly Journal of the Royal Meteorological Society*, 125:1407–1425.
- Tomažić, I., Le Borgne, P., and Roquet, H. (2014). Assessing the impact of brightness temperature simulation adjustment conditions in correcting Metop-A SST over the mediterranean sea. *Remote Sensing of Environment*, 146:214–233.
- Walton, C. C., Pichel, W. G., Sapper, J. F., and May, D. A. (1998). The development and operational application of nonlinear algorithms for the measurement of sea surface temperatures with the NOAA polar-orbiting environmental satellites. *Journal of Geophysical Research*, 103:27999–28012.